High Internal Phase Emulsion Ring-Opening Polymerization of Pentadecanolide: Strategy to Obtain Porous Scaffolds in a Single Step

Esha Sharma, Archana Samanta, Jit Pal, Supreet S. Bahga, Bhanu Nandan, Rajiv K. Srivastava*

Single-step process for production of porous scaffold based on poly(pentadecanolide) (PPDL) is reported. The scaffold is produced via in situ porosity generation during ring-opening polymerization (ROP) of the lactone pentadecanolide (PDL) in high internal phase emulsion (HIPE) using a water soluble enzyme (Lipase *TL*) as catalyst. The enzyme present in dispersed aqueous phase of HIPE effectively carries out ROP of monomer present in continuous oil phase. The polymerization occurs at the interface of oil and water in HIPE and complete monomer conversion is achieved in 96 h at 40 °C. Porous scaffold having interconnected pores is obtained as the final product and formation of PPDL is confirmed by spectroscopic and thermal analysis. The process thus developed is a single-step process to produce porous scaffolds via ROP of a lactone that can be extended to see its efficacy using monomer-soluble organometallic catalysts and monomers other than PDL including lactones, lactides, and cyclic carbonates.

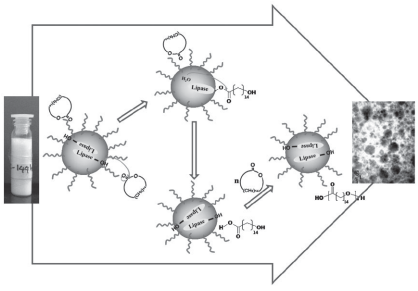

1. Introduction

Robust fabrication methods for reliable production of 3D porous scaffolds are in high demand due to huge potential that has been seen with application of 3D scaffolds in various areas specially tissue engineering.[1,2] 3D porous scaffolds are an absolute requirement for successful tissue engineering and the choice of scaffold material and its microstructure are prime parameters for an effective culture of artificial tissues.[3,4] The cell behavior is highly influenced by surface texture, pore size, and interconnectivity of the scaffold.[5–7] Selective adsorption, filtration and separation, catalysis, and energy storage are some other areas where use of porous scaffolds has been explored due to the advantage originating from their high surface area to mass ratio.[8–11]

There are many advanced techniques that have been adopted for producing 3D porous scaffolds today. Solid freeform fabrication (SFF) and rapid prototyping are the most common names given to a host of related technologies that are used to fabricate physical objects directly from computer aided data sources.[12–16] These methods are unique in that they add and bond materials in layers to form objects. Such systems are also known by the names additive fabrication, 3D printing or layered manufacturing.[8,17] Many of these advanced fabrication methods have been applied for the production of porous scaffolds. However all of these methods are multistep, require a preformed polymer and the

E. Sharma, A. Samanta, J. Pal, Dr. B. Nandan, Dr. R. K. Srivastava
Department of Textile Technology
Indian Institute of Technology Delhi
Hauz Khas, New Delhi 110016, India
E-mail: rajiv@textile.iitd.ac.in
Dr. S. S. Bahga
Department of Mechanical Engineering
Indian Institute of Technology Delhi
Hauz Khas, New Delhi 110016, India

Macromol. Chem. Phys. **2016**, DOI: 10.1002/macp.201600117

fabrication is carried at high temperatures. In addition to SFF techniques several fabrication methods that are based on organic solvents have also been used to prepare porous scaffolds.[18–20] The three most common are: Fiber bonding, phase separation, and solvent casting/particulate leaching.[21–23] These three techniques require the use of organic solvents, which could reduce the ability of cells to form new tissues in vivo.[24,25] Thus, long processing time to fully remove these solvents is necessary. In order to extract these chemicals, the scaffold must be vacuum dried for several hours, making it difficult to be used immediately in a clinical setting and requires added cost. The combination of toxic chemicals and extreme temperature presents difficulties if cells or bioactive molecules, such as growth factors, are to be included in the scaffold during processing. In addition, quality, speed, reproducibility, and scalability of these techniques are issues that still need to be addressed.

High internal phase emulsion (HIPE) is known for its excessive volume fraction of dispersed phase and polymerization of continuous phase of a HIPE was used as an effective approach to produce porous scaffolds via in situ generation of porosity during polymerization.[26–30] HIPE is characterized for its high volume fraction of dispersed phase (>0.74).[31,32] The work has so far been expanded for free-radical polymerization of variety of vinylic monomers forming the continuous phase of a water-in-oil HIPE.[33,34] The initiators (thermal as well as photoinitiators) used were monomer soluble and the scaffolds thus developed were characterized for their high porosity and interconnectedness of pores.[29] The work however has been limited to only vinylic monomers and ring-opening polymerization (ROP) of cyclic monomers including lactones or lactides has not been carried out in HIPE. Two prime reasons for this state were: (a) Sensitivity of monomers and catalysts toward moisture, (b) stability of emulsions, specially HIPEs, made using such monomers in water-in-oil emulsions. There are only handful of reports on polymerization of such monomers in a water-based emulsion system.[35–38] Moreover, the reports are only limited to formation of a conventional emulsion and its polymerization. Use of enzymes as catalyst under HIPE formulations has scantly been reported and the reactions were not polymerization.[39,40]

In the present approach, we worked toward developing a single-step, solvent-free process for creating a porous scaffold via polymerization of a lactone in HIPE formulation. The overall objective was to develop a stable HIPE for pentadecanolide (PDL) monomer in a water-in-oil emulsion that could later be efficiently polymerized to a 3D porous scaffold via in situ porosity generation during polymerization. The check on stability of HIPE was not limited to room temperature but extended to the temperature of polymerization, i.e., 40–60 °C. The lactone selected was PDL due to its high hydrophobicity in comparison to other small size lactones and better possibility for formation of a stable water-in-oil HIPE. The ROP was catalyzed using Lipase *TL* as the catalyst. PDL formed the continuous oil phase of HIPE in volume fraction = 0.26 while the catalyst was present in dispersed aqueous phase of volume fraction = 0.74. Polymerization was carried out at varied temperature and nature and concentration of catalyst and effect of these parameters on monomer conversion was evaluated.

2. Experimental Section

2.1. Materials

Pentadecalactone (purity>99.0%) was purchased from Sigma-Aldrich. Nonsoluble enzyme Novozyme-435 (Lipase *Candida antarctica*) Lipase B of activity ≥10 000 U g^{-1} (as reported by the supplier) immobilized on a macroporous support, Lewatit VPOC 1600 was a kind gift from Novozymes. Lipase *Thermomyces lanuginosus* (Lipase *TL*) having activity of ≥1 00 000 U g^{-1} (as reported by the supplier) was purchased in aqueous solution form from Sigma-Aldrich. The enzyme solution comprised of water (72% w/v), propylene glycol, and sorbitol (25% w/v), lipase (2% w/v), sodium benzoate (0.15% w/v), potassium sorbate (0.15% w/v), and calcium chloride (0.5% w/v). Deionized water (Millipore India), chloroform, deuterated chloroform, ethanol, dichloromethane (Merck India) were used as received. Span 80 (also known as sorbitane monooleate, a nonionic surfactant having molecular formula $C_{24}H_{44}O_6$) was purchased from Sigma-Aldrich.

2.2. Characterization

Proton nuclear magnetic spectroscopy (^{1}H-NMR) spectra were recorded in $CDCl_3$ using 300 MHz Bruker NMR spectrometer. Chemical shifts were reported in ppm relative to $CDCl_3$ ($\delta = 7.27$). Melting point and relative crystallinity of the polymer was determined using Perkin Elmer DSC differential scanning calorimeter (DSC) instrument and thermal stability of the polymer was assessed in a TA Instruments Q500 T (thermogravimetric analyzer (TGA) analyzer. Gel permeation chromatography (GPC) was performed in chloroform on a Verotech PL-GPC 50 Plus system equipped with a PL-RI detector and two PolarGel-M Organic (300 × 7.5 mm) columns from Varian. Scanning electron microscope (SEM) images were acquired using a Zeiss EVO 50 SEM on samples precoated with gold. Wide angle X-ray diffraction (WAXD) analysis was performed using PW3040/60 X'pert Pro instrument of PAN Analytical operating at 40 KV and 30 mA current at Kα, 1.54 A° wavelength, and 2θ range from 10° to 40°. Optical microscopic pictures were obtained using Nikon Eclipse E200 optical microscope in refractive mode. Gel content was determined gravimetrically.

2.3. General Procedure for Enzyme Catalyzed Interfacial HIPE-ROP

A predetermined amount of PDL monomer was taken in a vial along with the emulsifier Span 80 (50 wt% with respect

Macromol. Chem. Phys. **2016**, DOI: 10.1002/macp.201600117

Table 1. Formation of stable water-in-oil high internal phase emulsion of PDL.

Sample ID	PDL[a] [ml]	Enzyme		Temp [°C]	Monomer Conversion [%][d]	Time [h][e]	M_n [g mol^{-1}][f]	Polydispersity Index (PDI)[f]
		Nature[b]	[wt%][c]					
PDLH-1	2.6	Soluble	1.0	40	46	144	892	1.6
PDLH-2	2.6	Soluble	2.0	40	81	144	970	1.5
PDLH-3	2.6	Soluble	5.0	40	100	96	1515	1.2
PDLH-4	2.6	Insoluble	10.0	60	0	120	–	–

[a]PDL monomer containing 50 wt% of Span 80 comprised the continuous phase of HIPE; [b]Soluble enzyme: Aqueous Lipase *TL* solution. Insoluble enzyme: Novozyme-435; [c]With respect to PDL; [d]Obtained from ^{1}H-NMR; [e]Time of polymerization to obtain maximum monomer conversion within 6 d; [f]Values obtained from chloroform soluble fraction using GPC.

to monomer) and the mixture was stirred at 40 °C to make a clear solution (oil phase). Precalculated quantity of aqueous phase (containing adjusted amount of aqueous enzyme solution with respect to monomer) was added at controlled rate to the oil phase under high speed stirring. The volume fraction of dispersed aqueous (Φ_d) and continuous oil (Φ_c) phase was kept constant at 0.74 and 0.26, respectively. The HIPE thus formed was stirred for an additional hour and the polymerization was started by immersing the vial in an oil bath heated at controlled temperature using a thermocouple. Samples were withdrawn intermittently to determine monomer conversion. The polymerizations were continued for maximum 6 d and monomer conversion obtained within this period was reported for various samples. Polymer free from other reactants was obtained by dissolving the crude mixture in chloroform and precipitating in cold methanol. Effect of temperature, nature, and amount of enzyme was studied on monomer conversion and details are provided in Table 1.

3. Results and Discussion

HIPE of PDL forming the continuous phase was found to be stable at temperatures up to 60 °C and no phase separation was observed visually for over one week (Figure 1). The dispersed phase was formed by the aqueous enzyme solution and additional water to keep the volume fractions of dispersed aqueous (Φ_d) and continuous oil (Φ_c) phases at desired levels. The polymerization was first conducted at

Figure 1. Stable high internal phase emulsion of PDL.

40 °C at $\Phi_d/\Phi_c = 0.74/0.26$ and samples were withdrawn at regular intervals to determine monomer conversion using ^{1}H-NMR. It was observed while dissolving the crude reaction mixture in solvent (chloroform or deuterated chloroform) that a part of sample remained insoluble. The NMR was therefore performed on the filtrate after removal of the insoluble content of the sample. Disappearance of oxymethylene proton peak from monomer ($\delta = 4.05$ ppm) was taken as the completion of polymerization (Figure 2). A comparison of the intensity of oxymethylene proton peak originating from soluble polymer fraction ($\delta = 4.14$ ppm) and unreacted monomer ($\delta = 4.05$ ppm) was used to calculate the monomer conversion during polymerization. The monomer conversion values thus obtained were though not true representation of the polymer that was getting formed, as a fraction of polymer sample remained insoluble in the solvent and the extent of formation of insoluble content increased with time of polymerization.

ROP occurred at the interface of two phases as shown in scheme under table of content. The enzyme-activated monomer (EAM) complex was formed at the interface which led to formation of ring-opened monomer due to nucleophilic attack from the initiator, i.e., water. The polymer chain grew further via repetitive nucleophilic attack from hydroxyl end of the ring-opened monomer/oligomers on EAM complex. It was observed that a fraction of the sample taken out for NMR analysis remained insoluble in chloroform at room temperature. On the other hand, insoluble fraction immediately solubilized when the mixture was heated to 60 °C or few drops of trifluroacetic acid were added to the mixture. Thus, the insoluble fraction formed during polymerization was not a cross-linked polymer; possibility for formation of which anyway was remote as no cross-linking could have happened during polymerization based on the formulation selected. The insoluble portion thus formed could possibly be due to the initiation of ROP by stabilizers, viz., sorbitol and propylene glycol present in high quantity in the enzyme solution and trans-esterification occurring simultaneously (Scheme 1). A hyperbranched polymer

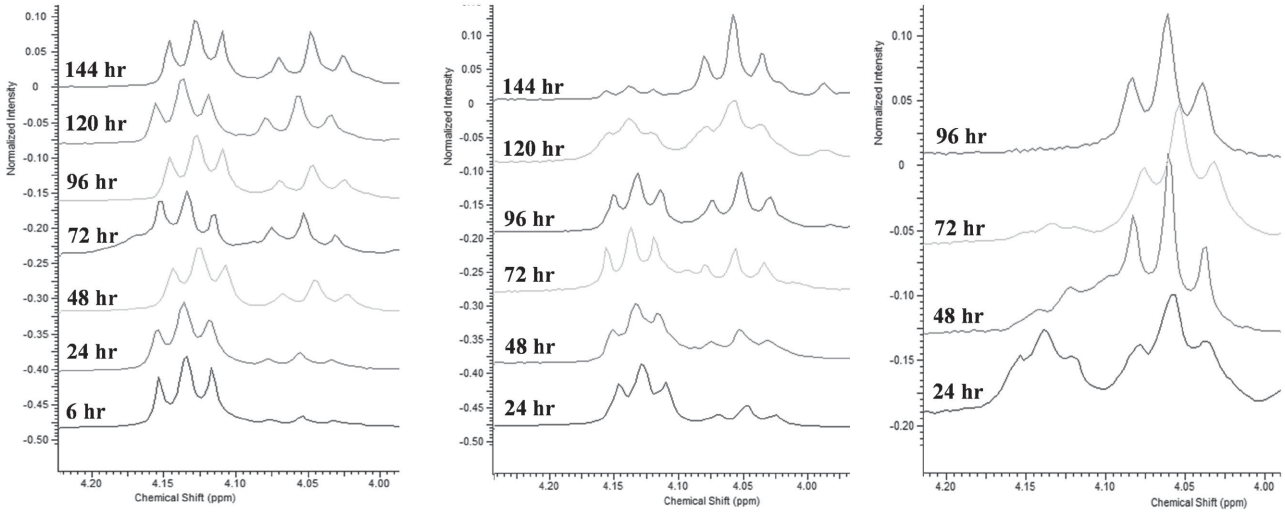

Figure 2. Change in intensity of oxymethylene protons of monomer (4.14 ppm) and polymer (4.05 ppm) with time a) PDLH-1, b) PDLH-2, and c) PDLH-3.

was therefore formed resulting into formation of a gel in chloroform at room temperature.

A higher monomer conversion was obtained using high amount of Lipase *TL* in the dispersed aqueous phase of HIPE when ROP was conducted at 40 °C (Table 1). A plot of monomer conversion with time using varying amounts of Lipase *TL* is shown in Figure 3. The rate of polymerization increased with increase in lipase concentration in aqueous phase, as expected. The apparent rates of polymerization calculated from linear fit of the data in Figure 3 were found to be 0.38, 0.56, and 1.16 sec^{-1} with Lipase *TL* amount of 1, 2, and 5 wt%, respectively. 100% monomer conversion was achieved in 96 h using 5 wt% of Lipase *TL* (with respect to monomer) at 40 °C. An increase in gel fraction was also seen as the polymerization progressed (Figure 3). Due to limited solubility of the sample in chloroform at room temperature, molecular weight determination using gel permeation chromatography could not be performed for all the samples. Values presented in Table 1 for poly(pentadecanolide) (PPDL) samples were obtained from GPC analysis of soluble fraction of the samples. Soluble fraction was obtained as filtrate after removal of insoluble part from the crude reaction mixture and the filtrate was later precipitated in cold methanol. The precipitated part of the sample was then redissolved in chloroform for GPC analysis. An increase in

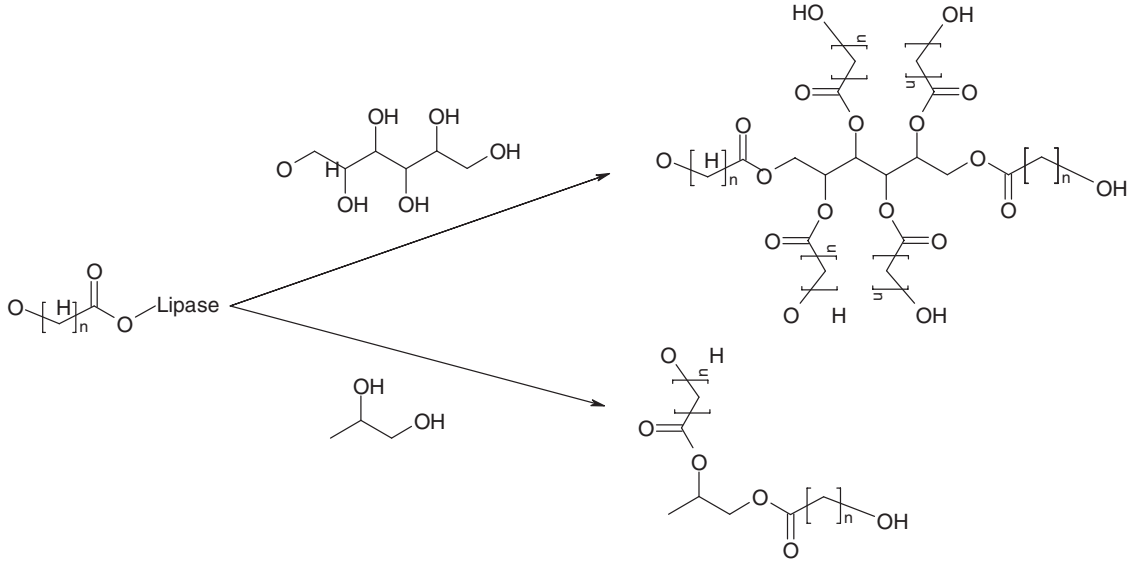

Scheme 1. Formation of hyperbranched PPDL via initiation of ROP from sorbitol and propylene glycol during HIPE-ROP of PDL.

Macromolecular Journals
Macromol. Chem. Phys. **2016**, DOI: 10.1002/macp.201600117

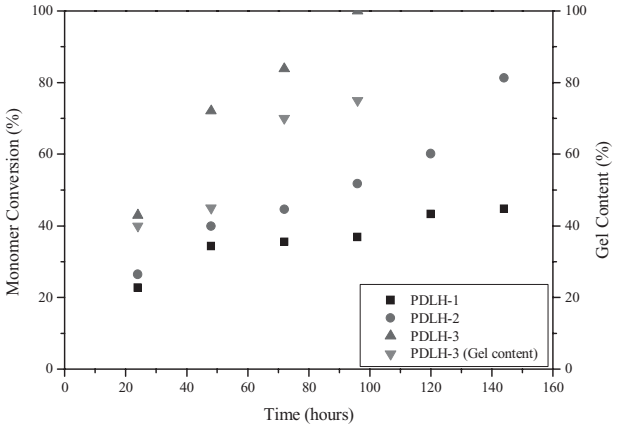

Figure 3. Monomer conversion with time using varying amount of Lipase *TL* for HIPE-ROP of PDL.

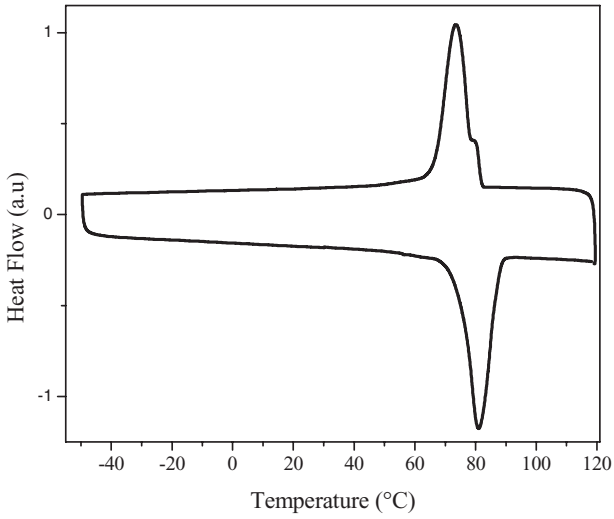

Figure 4. DSC thermogarm of PPDL synthesized via HIPE-ROP.

number average molecular weight (M_n) with increasing Lipase *TL* amount was observed, however, the readings could only be taken as representative values originating from soluble fraction of the polymer in chloroform. The trend could be taken as confirmation for formation of high-molecular-weight polymer with higher quantity of Lipase. The HIPE-ROP for PDL was also conducted in presence of an insoluble enzyme Lipase *CA* (Novozyme 435) which was present in dispersed aqueous phase. As expected, no monomer conversion was seen even when the polymerization was conducted at a slightly higher temperature, i.e., 60 °C.

Formation of PPDL was confirmed by thermal and WAXD analysis of ethanol washed samples. Crude polymer obtained after maximum monomer conversion that could be achieved within 6 d of polymerization was taken out and thoroughly washed with ethanol to remove all the enzyme, stabilizers, and emulsifier. DSC analysis of the dried, purified sample (PDLH-3) showed a melting peak at ≈81 °C and a relative crystallinity value of ≈45% calculated using heat of fusion of 100% crystalline PPDL[41] (Figure 4). TGA analysis of the polymer (PDLH-3) showed maximum degradation temperature at ≈405 °C (Figure 5) and peaks at $2\theta = 21°$ and 24° were obtained in WAXD measurement (Figure 6). All these values matched with previously reported values for PPDL in literature suggesting formation of high-molecular-weight polymer under HIPE-ROP conditions.

SEM pictures of the final polymer PDLH-3 synthesized via HIPE-ROP were obtained after thoroughly washing the samples with ethanol and drying under vacuum. No clear pores could be seen from the images for any of the samples rather a more flaky structure was obtained. This is because the glass transition of the PPDL polymer is much below room temperature (–27 °C) and by the time samples were dried and coated for SEM scanning, the structure was collapsed into more like a flaky structure. This observation however revealed the heterogeneity present in the polymerization mixture comprised in HIPE conditions and showed that the polymerization indeed occurred at the interface of oil and water phases thus producing thin flakes of the polymer at the interface. The SEM images are shown in Figure 7. Since clear porous structure could not be seen in SEM images of the PPDL samples, it was decided to capture the optical microscopic images under cryo-conditions by freezing

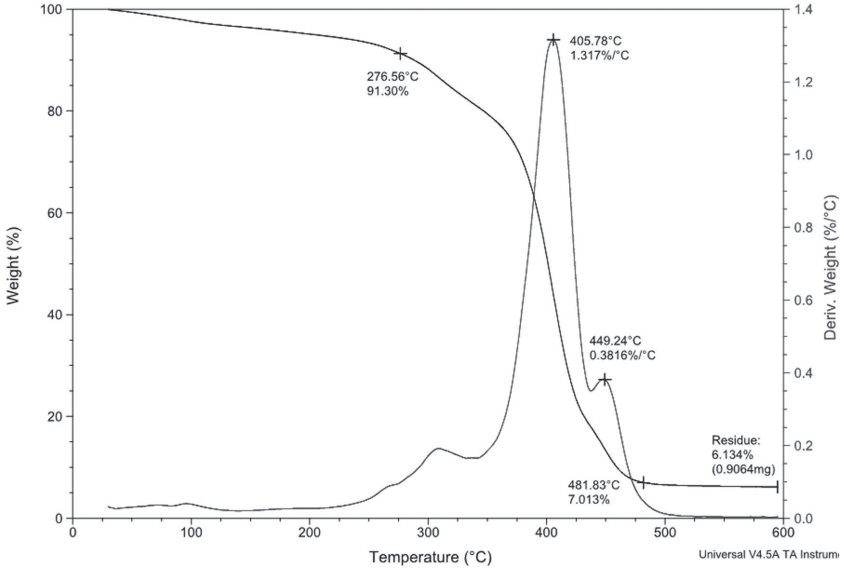

Figure 5. TGA plot of PPDL synthesized via HIPE-ROP.

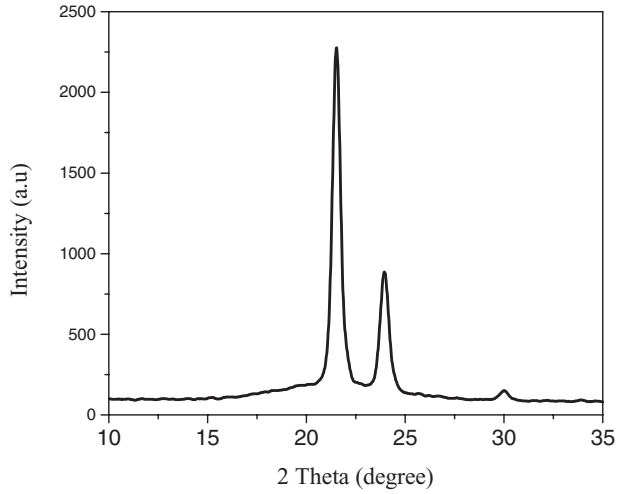

Figure 6. WAXD plot of PPDL synthesized via HIPE-ROP.

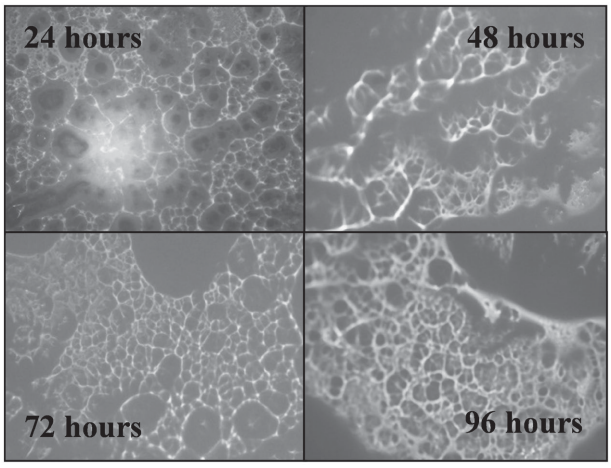

Figure 8. Optical microscopic images of PPDL synthesized via HIPE-ROP; samples analyzed at different time of polymerization.

the polymer in liquid nitrogen and taking pictures as soon as possible. A compiled view of pore formation for PDLH-3 is shown in Figure 8 when the polymer samples were taken at different intervals, frozen, and then images were taken under optical microscope. Porous structure having interconnected pores could be seen from the optical microscopic images thereby revealing a true HIPE structure that was formed under the chosen set of polymerization conditions and formulation. The disparity in pore size increased as the polymerization proceeded. In the SEM analysis no well-defined porous structure based on HIPE could be seen as the sample structure was collapsed after drying and coating. Also the samples polymerized in the vial were too thick to be seen under the optical microscope. Hence, the polymerization was later carried out on glass slides. The optical images of the polymer synthesized on glass slides are shown in Figure 9. A well-defined HIPE structure with interconnected pores was seen from the images obtained and the average pore size was found to be in the range of 30–70 microns.

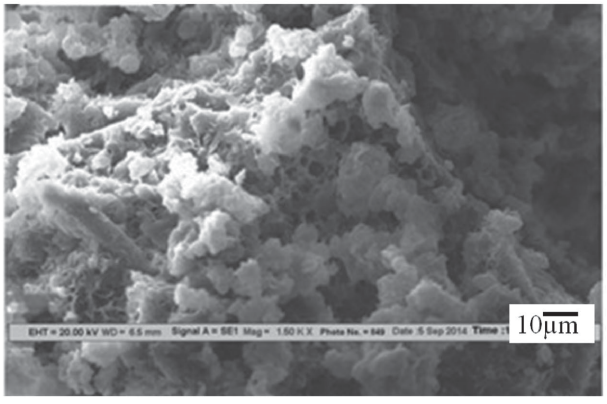

(a)

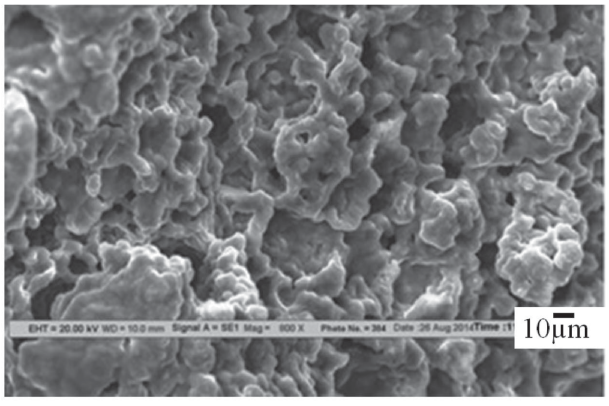

(b)

Figure 7. SEM images of PPDL synthesized via HIPE-ROP a) surface and b) cross-section.

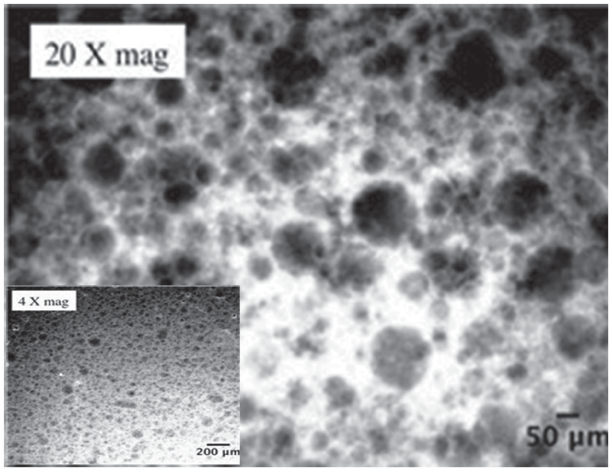

Figure 9. Optical microscopic images of PPDL synthesized via HIPE-ROP.

Macromol. Chem. Phys. **2016**, DOI: 10.1002/macp.201600117

Early View Publication; these are NOT the final page numbers, use DOI for citation !!

4. Conclusions

Water-in-oil HIPE of PDL was formed using Span80 as the emulsifier and the emulsion was found to be stable for more than a week at temperatures up to 60 °C. PDL present in volume fraction of 0.26 comprised the continuous phase of HIPE. ROP of PDL in HIPE was conducted at 40 °C using a water soluble enzyme Lipase *TL* as the catalyst. The enzyme was present in the dispersed phase and polymerization occurred at the interface of dispersed and continuous phases of emulsion. 100% monomer conversion was achieved at 40 °C in 96 h and the apparent rate of polymerization was found to increase with higher amount of Lipase *TL*. Formation of PPDL was confirmed by spectroscopic, thermal, and WAXD characterization. A fraction of polymer that remained insoluble in chloroform was due to initiation of ROP by sorbitol and propylene glycol present in the enzyme solution. Formation of pores and their interconnectedness was seen in the final polymer synthesized via HIPE-ROP of PDL. The method based on HIPE-ROP is a single-step process for generation of porous scaffold free from organic solvents and organometallic catalysts. The method may further be explored for polymerization of other lactones and lactides under HIPE conditions using catalysts other than enzymes and may become commercially viable for production of porous scaffolds fulfilling shortfalls of the existing scaffolding techniques.

Acknowledgement: Authors gratefully acknowledge the financial support provided by Indian Institute of Technology Delhi and Department of Science and Technology India (Grant No. SERB/F/3988/2014-15) to perform this research.

Received: March 15, 2016; Revised: April 19, 2016; Published online: ; DOI: 10.1002/macp.201600117

Keywords: enzyme; HIPE; pentadecanolide; porous; ROP; scaffold

[1] D. W. Hutmacher, M. Sittinger, M. V. Risbud, *Trends Biotechnol.* **2004**, *22*, 354.
[2] J. L. Drury, D. J. Mooney, *Biomaterials* **2003**, *24*, 4337.
[3] V. Karageorgiou, D. Kaplan, *Biomaterials* **2005**, *26*, 5474.
[4] A. V. Janorkar, in *Biomaterials* (Eds: A. S. Kulshrestha, A. Mahapatro, L. A. Henderson), American Chemical Society, Washington, DC **2010**, pp. 1–32.
[5] J. Fox, *Chem. Eng. News* **1980**, *58*, 36.
[6] S. J. Hollister, *Nat. Mater.* **2005**, *4*, 518.
[7] K. Xu, Q. Shuai, X. Li, Y. Zhang, C. Gao, L. Cao, F. Hu, T. Akaike, J. Wang, Z. Gu, J. Yang, *Biomacromolecules* **2016**, *17*, 756.
[8] D. Singh, D. Singh, S. Han, *Polymers* **2016**, *8*, 19.
[9] Q. P. Pham, U. Sharma, A. G. Mikos, *Biomacromolecules* **2006**, *7*, 2796.
[10] J.-R. Li, J. Yu, W. Lu, L.-B. Sun, J. Sculley, P. B. Balbuena, H.-C. Zhou, *Nat. Commun.* **2013**, *4*, 1538.
[11] Y. Gao, T. Mori, S. Manning, Y. Zhao, A. d. Nielsen, A. Neshat, A. Sharma, C. J. Mahnen, H. R. Everson, S. Crotty, R. J. Clements, C. Malcuit, E. Hegmann, *ACS Macro Lett.* **2016**, *5*, 4.
[12] P. B. Allen, Z. Khaing, C. E. Schmidt, A. D. Ellington, *ACS Biomater. Sci. Eng.* **2015**, *1*, 19.
[13] L. R. Hart, S. Li, C. Sturgess, R. Wildman, J. R. Jones, W. Hayes, *ACS Appl. Mater. Interfaces* **2016**, *8*, 3115.
[14] M. Hofmann, *ACS Macro Lett.* **2014**, *3*, 382.
[15] Y. A. Abramov, *Org. Process Res. Dev.* **2013**, *17*, 472.
[16] D. Yang, H. Hong, Y. H. Seo, L. H. Kim, W. Ryu, *ACS Appl. Mater. Interfaces* **2015**, *7*, 16873.
[17] V. N. Truskett, M. P. C. Watts, *Trends Biotechnol.* **2006**, *24*, 312.
[18] M. Zhang, A. Vora, W. Han, R. J. Wojtecki, H. Maune, A. B. A. Le, L. E. Thompson, G. M. McClelland, F. Ribet, A. C. Engler, A. Nelson, *Macromolecules* **2015**, *48*, 6482.
[19] P. Calvert, R. Crockett, *Chem. Mater.* **1997**, *9*, 650.
[20] S. Kumar, M. Hofmann, B. Steinmann, E. J. Foster, C. Weder, *ACS Appl. Mater. Interfaces* **2012**, *4*, 5399.
[21] D. Sin, X. Miao, G. Liu, F. Wei, G. Chadwick, C. Yan, T. Friis, *Mater. Sci. Eng. C* **2010**, *30*, 78.
[22] N. Thadavirul, P. Pavasant, P. Supaphol, *J. Biomed. Mater. Res. A* **2014**, *102*, 3379.
[23] X. Jing, H.-Y. Mi, T. Cordie, M. Salick, X.-F. Peng, L.-S. Turng, *Ind. Eng. Chem. Res.* **2014**, *53*, 17909.
[24] A. G. Mikos, J. S. Temenoff, *Electron. J. Biotechnol.* **2000**, *3*, NA.
[25] X. Wang, W. Li, V. Kumar, *Biomaterials* **2006**, *27*, 1924.
[26] N. R. Cameron, *Polymer* **2005**, *46*, 1439.
[27] N. R. Cameron, *J. Chromatogr. Libr.* **2003**, 255.
[28] N. R. Cameron, D. C. Sherrington, in *Biopolymers Liquid Crystalline Polymers Phase Emulsion*, Springer, Berlin Heidelberg **1996**, pp. 163–214.
[29] I. Pulko, P. Krajnc, *Macromol. Rapid Commun.* **2012**, *33*, 1731.
[30] P. Becher, *J. Dispersion Sci. Technol.* **1985**, *6*, 147.
[31] L. L. C. Wong, P. M. Baiz Villafranca, A. Menner, A. Bismarck, *Langmuir* **2013**, *29*, 5952.
[32] X. Li, G. Sun, Y. Li, J. C. Yu, J. Wu, G.-H. Ma, T. Ngai, *Langmuir* **2014**, *30*, 2676.
[33] H. Xu, X. Zheng, Y. Huang, H. Wang, Q. Du, *Langmuir* **2016**, *32*, 38.
[34] F. Svec, *J. Chromatogr. A* **2010**, *1217*, 902.
[35] S. Sosnowski, M. Gadzinowski, S. Slomkowski, *Macromolecules* **1996**, *29*, 4556.
[36] M. Gadzinowski, S. Sosnowski, S. Slomkowski, *Macromolecules* **1996**, *29*, 6404.
[37] A. Taden, M. Antonietti, K. Landfester, *Macromol. Rapid Commun.* **2003**, *24*, 512.
[38] S. Målberg, A. Finne-Wistrand, A.-C. Albertsson, *Polymer* **2010**, *51*, 5318.
[39] L. Espelt, P. Clapés, J. Esquena, A. Manich, C. Solans, *Langmuir* **2003**, *19*, 1337.
[40] A. Barbetta, M. Massimi, L. Conti Devirgiliis, M. Dentini, *Biomacromolecules* **2006**, *7*, 3059.
[41] M. Letizia Focarete, M. Scandola, A. Kumar, R. A. Gross, *J. Polym. Sci. Part B: Polym. Phys.* **2001**, *39*, 1721.